JVSTB Journal of Vacuum Science & Technology B

Large area infrared frequency selective surface with dimensions reproducible by optical lithography

Jeffrey A. D' Archangel, David J. Shelton, Robert Hudgins, Menelaos K. Poutous, and Glenn D. Boreman

Citation: Journal of Vacuum Science & Technology B **32**, 051807 (2014); doi: 10.1116/1.4895663
View online: http://dx.doi.org/10.1116/1.4895663
View Table of Contents: http://scitation.aip.org/content/avs/journal/jvstb/32/5?ver=pdfcov
Published by the AVS: Science & Technology of Materials, Interfaces, and Processing

Large area infrared frequency selective surface with dimensions reproducible by optical lithography

Jeffrey A. D' Archangel
CREOL, The College of Optics and Photonics, University of Central Florida, 4304 Scorpius St., Orlando, Florida 32816

David J. Shelton
Plasmonics Inc., 12565 Research Parkway, Suite 300, Orlando, Florida 32826

Robert Hudgins
Center for Optoelectronics and Optical Communications, University of North Carolina at Charlotte, 9201 University City Blvd., Charlotte, North Carolina 28223

Menelaos K. Poutous and Glenn D. Boreman[a)]
Department of Physics and Optical Science, University of North Carolina at Charlotte, 9201 University City Blvd., Charlotte, North Carolina 28223

(Received 27 May 2014; accepted 2 September 2014; published 16 September 2014)

An infrared frequency selective surface (FSS) with absorptive resonance near 6.5 μm was fabricated by electron-beam lithography using a patch design with dimensions reproducible by optical-projection lithography. By selective wet etching along with reactive-ion etching, the sample was divided into miniature FSS particles, which were released from the substrate. A large number of such particles could be implemented as a large area, conformal coating. Spectral reflectivity of the full FSS array as well as the FSS particles was measured and compared to electromagnetic simulations. To show the feasibility of this approach, the full array FSS design was fabricated using a g-line ($\lambda = 436$ nm) 5× projection lithography stepper and compared to the array fabricated by electron-beam lithography using scanning electron microscopy and Fourier transform infrared spectroscopy. Even though the resolution of the g-line stepper led to a poor fabrication output, the optical resonance was found to be robust, with only slight detuning attributed to the changes in unit cell geometry. This work highlights the utility of optical-projection lithography, coupled with the releasable particle fabrication procedure, to create a large area, conformal coating with specific infrared spectral properties.
[http://dx.doi.org/10.1116/1.4895663]

I. INTRODUCTION

Frequency selective surfaces (FSSs) have generated much interest at infrared wavelengths due to their ability to control spectral properties via electromagnetic resonance.[1–4] With spectral properties determined by subwavelength structures within an array, FSS are often referred to as metamaterials or metasurfaces. The sub-μm dimensions required for infrared FSS typically dictate fabrication on rigid substrates for compatibility with standardized lithographic and thin-film processing equipment. The utility of infrared FSS has been somewhat restricted by the size and rigidity of the substrate, which is normally a standard semiconductor wafer. In addition, the practicality of applications using infrared FSS is often overshadowed by the presumed need for expensive and/or complex lithographic processing such as electron-beam lithography,[5] nanoimprint lithography,[5] and optical lithography with microlens projection[6] or phase-shift masks,[7] although fabrication of simple patch elements has previously been demonstrated using standard photolithography techniques.[8]

Recent efforts have shown that infrared FSS fabricated by electron-beam lithography may be released from a substrate in the form of miniature arrays, which retain most of the spectral characteristics of the full array, giving rise to the possibility of implementing such FSS particles in a large area, conformal infrared coating.[9] However, the speed of electron-beam lithography is impractical for the creation of a coating which is truly large in area. Here, a square patch infrared FSS has been designed and fabricated by electron-beam lithography, using feature sizes within the capability of optical projection lithography. The prospect of fabrication via optical lithography implies greatly increased throughput and lower production cost. In addition, the present work includes a process for FSS particle fabrication has been significantly improved through the use of a directional reactive-ion etcher (RIE). Through FTIR measurements, the spectral reflectivity of the fabricated miniature arrays is shown to compare favorably with that of the undivided array as well as electromagnetic simulations, when the fill factor of the FSS particles is taken into account. As a test of the resilience of the infrared FSS design with respect to the lower resolution of many optical lithography techniques, the full array FSS design was fabricated using a g-line ($\lambda = 436$ nm) stepper. Comparing the spectral reflectivity of the FSS fabricated by UV projection lithography and by electron-beam lithography, we demonstrate the feasibility of optical projection

a)Electronic mail: gboreman@uncc.edu

lithography for the fabrication of FSS structures with resonance in the 4–12 μm infrared wavelength range.

II. MODELING AND SIMULATION

As a design goal, the infrared FSS in this work was constructed of dimensions reproducible with a g-line stepper, typically capable of sub-μm resolution.[10] The g-line stepper was chosen because it represents the lower range in resolution among the existing stepper tools, making the FSS design demonstrated here widely adaptable. Since the line width requirement for infrared FSS is normally smaller than 0.5 μm, only the patch-type FSS elements could be considered. The design in this case was a square patch array encased in dielectric with a ground plane reflector. This design form resonates strongly when modes are set up between the conductive patches and the ground plane. In this work, the square patch elements were made of Au, the dielectric material consisted of benzocyclobutene (BCB) (Cyclotene 3022, The Dow Chemical Company), and the ground plane was Cr. BCB is a preferred dielectric for the FSS particle designs due to relative transparency over much of the infrared range as well as the ease by which it is etched by plasma processes.

Simulations were carried out in ANSYS HFSS, a 3D full-wave electromagnetic solver which uses the finite-element method. The FSS was simulated as an infinite array using the Floquet port approach and spectral reflectivity was obtained via a frequency sweep through calculation of the S-parameters. Since material properties show significant dispersion in the infrared,[11] the frequency dependent optical constants for the constituent materials were determined by ellipsometry and input into the simulation. The FSS particles were fabricated with symmetry about the ground plane such that either side yields the same electromagnetic response. The 150 nm Cr ground plane is considered to be optically thick such that only the top half of the structure needed to be simulated. The geometrical parameters of the FSS were iterated in the simulation to give a strong resonance (minima in reflectivity) near 6.5 μm and high reflectivity in other portions of the 4–12 μm range. The optimum simulated results were observed when the square patch side length was 1.28 μm, the thickness of the Au patch was 60 nm, the thickness of the BCB layer under the patch was 0.22 μm, and the thickness of the BCB overcoat was 0.18 μm. The periodicity of the elements was 2.07 μm such that the spacing in between subsequent patches was 0.79 μm, representing the critical dimension to be reproduced by lithography.

III. FABRICATION AND CHARACTERIZATION

The fabrication process for releasable FSS particles has been reported previously in detail[9] and will be summarized briefly here. For reference, a cross-sectional schematic showing two FSS particles before and after each step in the etching process is shown in Fig. 1. FSS arrays of area 5×5 mm were created on SiO_2 coated Si wafers using electron-beam lithography, metallization, and liftoff. The defined particle (subarray) dimensions were 20×20 μm. The SiO_2 acts as a sacrificial layer for the eventual release of the FSS particles from the substrate. The lithography was performed using a Leica EBPG5000+ electron-beam lithography system with ZEP 520A-7 electron-beam resist. The BCB layers were applied by spin coating, while the sacrificial SiO_2, Au elements, and Cr ground plane were deposited by electron-beam evaporation. Good adhesion of Au to BCB was achieved with a 5 nm Ti seed layer. The fact that the structure was fabricated with symmetry about the ground plane made the spectral response independent of the final face-up/face-down orientation of the particles and also robust to particle stacking effects due to the opaque ground plane.

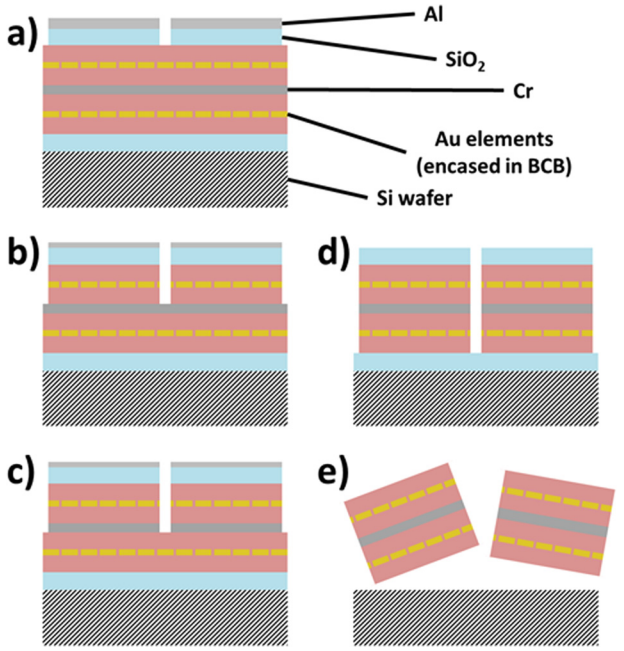

FIG. 1. (Color online) Cross-sectional schematic of two FSS particles, showing the constituent layers (a) as fabricated before etching, (b) after the first plasma etch of BCB, (c) after the wet etch of the Cr ground plane, (d) after the second plasma etch of BCB, and (e) after the hard mask and sacrificial layer of SiO_2 have been dissolved, releasing the particles from the substrate.

The size and shape of the particles was defined by a hard mask fabricated on top of the array, as can be seen in Fig. 1. Previously, the areas of BCB and FSS elements in between the defined particles were etched away using a barrel-type plasma etcher (Branson P2000) in a CF_4 and O_2 environment.[9] This isotropic etching step has been greatly improved with a much more directional plasma etcher, using a mixture of O_2 and SF_6 in a ratio of 17:8 and operating in RIE mode (Advanced Oxide Etcher, Surface Technology Systems). The hard mask was composed of SiO_2 and Al; in the experiments reported here, the Al mask was slowly etched away leaving a portion of the SiO_2 mask in place at the end of the RIE process. The Cr ground plane along the centerline of the flakes was wet etched as an intermediate step (Chrome Etch, Ashland Specialty Chemical Company). The sample was then placed in buffered-oxide etch (BOE) which dissolved the sacrificial SiO_2 layer as well as any remaining etch mask. This process released the particles from the substrate, where they were collected by drawing the solution through a filtered syringe. Next, the filter was pressed against a clean

Si wafer, transferring most of the FSS particles for further characterization. The sample was then placed on a 180 °C hot plate for a few seconds to remove any liquid residues remaining from the BOE solution.

Spectral characterization was carried out with a Perkin–Elmer microscope FTIR, measuring areas of the sample 100 μm in diameter. Measurements were made of the full FSS array (before fabrication of the etch mask) as well as collections of FSS particles. The measurement area of the FSS particles had an altered reflectivity due to the background of the Si collection wafer. To account for the Si background, the spectral reflectivity of the wafer was measured at a location far away from the FSS particles. Using the measured Si background reflectivity and measured full array FSS reflectivity, the expected spectral reflectivity of the sample areas containing FSS particles can be approximated as follows:

$$\rho_{\text{particles}} = f \cdot \rho_{\text{FSS}} + (1 - f) \cdot \rho_{\text{Si}}. \quad (1)$$

Here, $\rho_{\text{particles}}$ denotes the approximated spectral reflectivity of the FSS particles on the Si wafer, ρ_{FSS} denotes the measured spectral reflectivity of the original FSS array, ρ_{Si} denotes the measured spectral reflectivity of the Si collection wafer, and f is the fill factor of FSS particles on the bare Si wafer, defined as the proportion of the measurement area containing FSS particles. The fill factor can be estimated using SEM images or by fitting the experimental data to Eq. (1). Although it serves as a good approximation, it is noted that Eq. (1) is merely a linear combination of the FSS particles and Si background, which ignores the effects of array truncation.

IV. RESULTS AND DISCUSSION

The fabricated particles were imaged using SEM with a secondary electron detector to minimize the effects of charging. One such image is shown in Fig. 2, which depicts a small collection of FSS particles. As can be seen in the figure, the fabricated particles are square with relatively straight edges. This is in stark contrast to the previous work, where for samples including a ground plane, the edges were jagged and the size of the particles was irregular.[9] The improvement can be directly attributed to the process change for the etching of BCB, which was previously isotropic and is now much more directional. Additionally, the new etch process has allowed removal of the elements in between the masked off regions as well. This represents a significant improvement, since previously the FTIR measurement area was cluttered with stray Au debris.

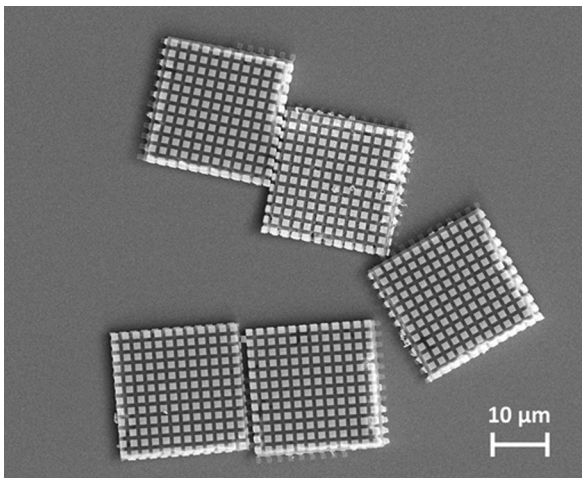

FIG. 2. SEM micrograph showing a small collection of FSS particles.

The spectral reflectivity the full FSS array as measured via FTIR is compared to the simulated reflectivity of the array in the top graph of Fig. 3. The bottom graph in Fig. 3 shows the measured reflectivity of the FSS particles and the best fit of Eq. (1) to the spectral shape of the FSS particle reflectivity. Note the difference in scaling between the top and bottom graphs. As can be seen in the figure, the measured and simulated data sets have spectral features which are quite similar for the majority of the 4–12 μm band. Both the full array and flake reflectivity data sets show a minima in reflectivity, corresponding to the resonant wavelength of the square patch FSS. The dip in reflectivity for the full array appears at approximately 6.4 μm, while the dip corresponding to the particle reflectivity appears at approximately 6.2 μm. This shift in resonant wavelength upon array truncation is due to

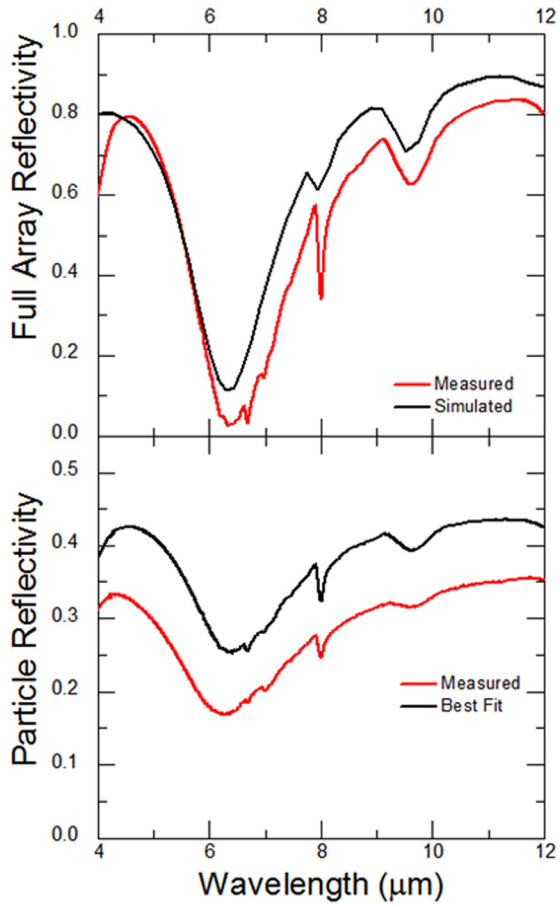

FIG. 3. (Color online) (Top) Measured reflectivity and simulated reflectivity of the full FSS array. (Bottom) Measured reflectivity of the FSS particles and calculated reflectivity using the minimized mean square fit of Eq. (1), which is a linear combination of the full FSS array and Si collection wafer reflectivity. Note the difference in scaling of the vertical axes between the top and bottom.

the lack of mutual coupling experienced by the edge elements, consistent with previous studies.[12] The absorption features near 8 and 9.5 μm are due to loss bands in BCB.[13,14]

The need for scaling the particle reflectivity measurement is primarily a result of the lack of particles filling the FTIR measurement area. The fill factor is determined by the distribution of flakes, which are collected by the filtered syringe and the amount of these which are transferred to the Si wafer for measurement. Due to the small amounts of source material (the initial full FSS array) and the laboratory scale collection routine, the distribution of FSS particles is quite random. In the discussion of fill factor, it is important to consider the possible effects that may occur when the distribution of the FSS particles causes them to be stacked upon each other. The utilization of ground plane symmetry in the design alleviates much of the concern, since only the top layer FSS contributes to the optical response. However, it is noted that with improvements in the FSS particle collection or overall throughput, a much larger fill factor will cause spectral effects because the stacking of many particles will undoubtedly lead to a random angular distribution with respect to the surface normal. It is expected that these issues could be alleviated by designing the FSS to have a fairly omnidirectional spectral response. It is noted that stacking effects were not observed here due to the sparse distribution of FSS particles.

The fitted plot in the bottom graph of Fig. 3 best matches the spectral shape of the FSS particle reflectivity measurement when the fill factor term in Eq. (1) is set to 0.22; this was determined by minimizing the summed mean-squared difference between the two plots while iterating the fill factor value. The fill factor was also inferred from several SEM images by adding a grid and counting the proportion of the field covered in FSS particles; these counts approximate the fill factor between 0.25 and 0.35. The measured reflectivity in the bottom plot of Fig. 3 is on average 9.1% lower than predicted by the fill factor, and diverges most near the resonant condition. The slight difference between the measured FSS particle reflectivity and that which is predicted by Eq. (1) can be attributed to multiple factors. First, the etch process, which releases the particles from the substrate, causes pitting in the BCB surfaces, as evidenced in Fig. 4, an SEM micrograph showing the edge of an FSS particle. The pitting is a result of a minor overexposure of the BCB surfaces to BOE, which can happen on the top side of all of the FSS particles if the SiO_2 mask is etched completely before the particles are released. The pitting also occurs on the underside of the particles, since the BOE etches the adjacent areas between the particles in the sacrificial layer first and then moves toward the center of the particles. The added surface roughness is thought to lead to a decreased specular reflectivity as measured by the FTIR microscope. Additionally, because the BOE solution containing FSS particles evaporates on the Si wafer, some contamination is likely left on the wafer near the FSS particles. This lack of local cleanliness may lead to a reduced Si reflectivity compared to the clean background measurement, which could contribute to a lower than expected overall measured reflectivity of the areas containing FSS particles. Furthermore, since the changes in behavior of the resonant condition upon array truncation are not predicted by the linear combination expressed in Eq. (1), the spectral region near resonance experiences an enhanced discrepancy between the measured and approximated FSS flake reflectivity data.

To provide experimental demonstration of the feasibility of optical-projection lithography as a fabrication method for infrared FSS structures, fabrication of the full FSS array was carried out using a 5× reduction g-line optical stepper (GCA 6300 C DSW Wafer Stepper). The full array square patch design was implemented in a 5× reticle and a 540 nm layer of S1805 was used as photoresist. Figure 5 compares the results of the full array FSS as fabricated by optical-projection lithography and electron-beam lithography in terms of spectral reflectivity and geometry. The SEM micrograph inset in the lower right of the figure depicts the results of this fabrication (left) as well as that of the full FSS array fabricated by electron-beam lithography before it was etched to create particles (right). As can be seen in the inset, the main difference between the fabrication techniques is that the square patches fabricated by optical-projection lithography show very

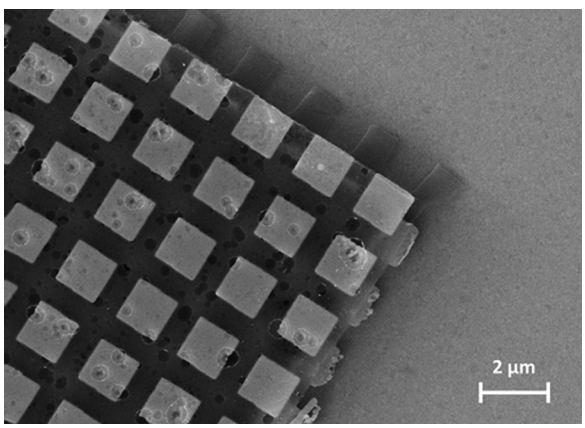

FIG. 4. SEM micrograph showing porosity in the surface of a FSS particle.

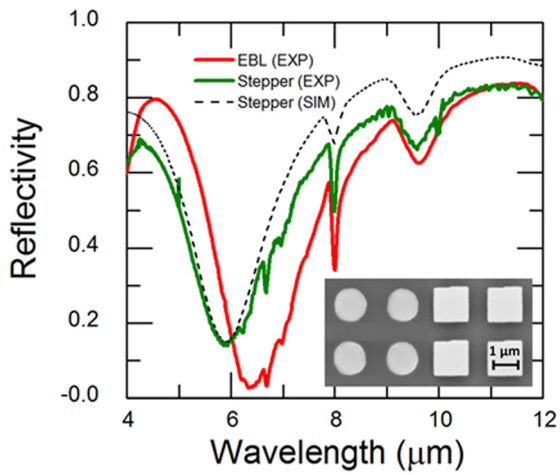

FIG. 5. (Color online) Measured reflectivity of the full FSS array as fabricated by electron-beam lithography, along with measured and simulated reflectivity of the full FSS array as fabricating using 5× g-line optical-projection lithography. The inset figure in the lower right corner is an SEM micrograph comparison of FSS arrays fabricated by g-line optical-projection lithography (left) vs electron-beam lithography (right).

rounded corners, while the patches fabricated by electron-beam lithography are reasonably square. The patch size and spacing between adjacent patches is held relatively consistent between the two fabrication techniques.

As can be seen in the spectral reflectivity comparison of Fig. 5, the rounded corners of the lower resolution stepper fabrication result in a slight blue-shifting of the resonant wavelength as well as a small reduction in the strength of resonance. The resonant wavelength of a square patch varies proportionally to the length of its sides. Since the rounded corners reduce the effective size of the patches, the resonant wavelength blue-shifts accordingly. Showing a good qualitative match, simulation of the projection lithography array was performed using the observed geometry of the fabrication, including the addition of a 0.4 μm radius of curvature to the square edges. It is noted that the optical resonance of the FSS design is observed to be robust even though the resolution of the g-line technique is poor. This result gives immense confidence toward the fabrication of plate-type infrared FSS designs using optical projection lithography, especially at exposure wavelengths shorter than 436 nm.

The rounded corners observed in the g-line stepper fabrication are a result of the resolution limits of this lithographic technique, which was chosen to illustrate the results of optical lithography with poor resolution on the spectral reflectivity of the infrared FSS. For g-line stepper fabrication, iteration of the lithographic processing by varying the exposure time, focus, and resist properties may reduce the roundness of the corners. Moreover, the addition of serifs (corner protrusions) as a form of optical proximity correction on the reticle would sharpen the edges considerably.[15] It is additionally noted that by consideration of the resolution limits of g-line optical-projection lithography, the FSS could be redesigned using rounded patches, and by tuning other parameters such as the periodicity, element size, and the thickness of the dielectric layers to optimize a resonance at a given design wavelength. Furthermore, utilization of more modern optical projection tools with shorter wavelength exposure sources such as i-line ($\lambda = 365$ nm), KrF ($\lambda = 248$ nm), and ArF ($\lambda = 193$ nm) would lead to more accurate replication of the FSS design as compared to the g-line stepper used here, with the KrF and ArF tools likely capable of producing infrared patch FSS, which are almost identical to those fabricated by electron-beam lithography.

V. SUMMARY AND CONCLUSIONS

An infrared FSS was designed with an absorptive resonance near 6.5 μm, and fabricated using both UV projection-lithography and electron-beam lithography. The array fabricated by electron-beam lithography was transformed into FSS particles by an etching process that defines the particles as subarrays and releases them from the substrate. The use of RIE for the plasma etching step represents an improvement over a previously presented method in terms of FSS particle definition as well as fabrication cleanliness. The spectral reflectivity, which was measured via FTIR, shows comparable spectral features between the full FSS array and the FSS particles. The biggest difference between the two is the amplitude and spectral position of the resonant absorptive feature, which can be attributed to the fill factor of FSS particles in the measurement area and array truncation effects, respectively. The full FSS array was also fabricated by optical-projection lithography using a g-line 5× reduction stepper. While the poor resolution of the g-line tool led to almost circular elements, measurements show that the absorptive resonance of the array was robust to these effects, as the minima in reflectivity was only slightly detuned toward shorter wavelengths. The detuning could be corrected for in the design and fabrication allowing for the resonance to be placed at a given wavelength. Alternatively, a stepper tool with shorter exposure wavelength could be utilized to much more precisely replicate the original design.

ACKNOWLEDGMENTS

Portions of this research were supported by the Laboratory Directed Research and Development program at Sandia National Laboratories. Sandia National Laboratories is a multi-program laboratory managed and operated by Sandia Corporation, a wholly owned subsidiary of Lockheed Martin Corporation, for the U.S. Department of Energy's National Nuclear Security Administration under Contract No. DE-AC04-94AL85000. Portions of this work were supported by the National Science Foundation under Grant No. 1068050. J.D. gratefully acknowledges support from the SMART Scholarship, funded by OSD-T&E (Office of Secretary Defense-Test and Evaluation), Defense –Wide/PE0601120D8Z National Defense Education Program (NDEP)/BA-1, Basic Research. The authors acknowledge the anonymous reviewers who have enhanced the quality of this manuscript.

[1]I. Puscasu, W. L. Schaich, and G. D. Boreman, IR Phys. Technol. **43**, 101 (2002).
[2]R. T. Kristenses, J. F. Beausang, and D. M. DePoy, J. Appl. Phys. **95**, 4845 (2004).
[3]J. A. Bossard, D. H. Werner, T. S. Mayer, J. A. Smith, Y. U. Tang, R. P. Drupp, and L. Li, IEEE Trans. Antennas Propag. **54**, 1265 (2006).
[4]X. Liu, T. Tyler, T. Starr, A. F. Starr, N. M. Jokerst, and W. J. Padilla, Phys. Rev. Lett. **107**, 045901 (2011).
[5]I. Puscasu, G. D. Boreman, R. C. Tiberio, D. Spencer, and R. R. Krchnavek, J. Vac. Sci. Technol., B **18**, 3578 (2000).
[6]M. H. Wu, K. E. Paul, J. Yang, and G. M. Whitesides, Appl. Phys. Lett. **80**, 3500 (2002).
[7]S. J. Spector, D. K. Astolfi, S. P. Doran, T. M. Lyszczarz, and J. E. Raynolds, J. Vac. Sci. Technol., B **19**, 2757 (2001).
[8]T. Schimert, M. E. Kock, and C. H. Chan, J. Opt. Soc. Am. A **7**, 1545 (1990).
[9]J. A. D' Archangel, G. D. Boreman, D. J. Shelton, M. B. Sinclair, and I. Brener, J. Vac. Sci. Technol., B **29**, 051806 (2011).
[10]S. A. Campbell, *The Science and Engineering of Microelectronic Fabrication* (Oxford University, New York, 2001).
[11]F. J. González, J. Alda, J. Simón, J. Ginn, and G. Boreman, IR Phys. Technol. **52**, 48 (2009).
[12]J. D' Archangel, E. Tucker, M. B. Raschke, and G. Boreman, Opt. Express **22**, 16645 (2014).
[13]J. T. Beechinoor, E. McGlynn, M. O'Rielly, and G. M. Crean, Microelectron. Eng. **33**, 363 (1997).
[14]W. R. Folks, J. Ginn, D. J. Shelton, J. Tharp, and G. D. Boreman, Phys. Status Solidi C **5**, 1113 (2008).
[15]A. K. K. Wong, *Resolution Enhancement Techniques in Optical Lithography* (SPIE, Bellingham, WA, 2001).